

Electron and Photon Performance and Electron p_T Spectrum Measurement with ATLAS in pp Collisions at $\sqrt{s} = 7$ TeV

Scott Snyder*

(For the ATLAS Collaboration)

Brookhaven National Laboratory (BNL)

E-mail: snyder@bnl.gov

We discuss the early performance of the reconstruction of electrons and photons at ATLAS with a center-of-mass energy of 7 TeV. Using a data sample of about 15 nb^{-1} , we present a measurement of the transverse momentum distribution of inclusive electrons, as well as an observation of prompt photons and a measurement of the purity of this sample. We also demonstrate the reconstruction of J/ψ mesons with a data sample of 78 nb^{-1} .

35th International Conference of High Energy Physics
July 22-28, 2010
Paris, France

*Speaker.



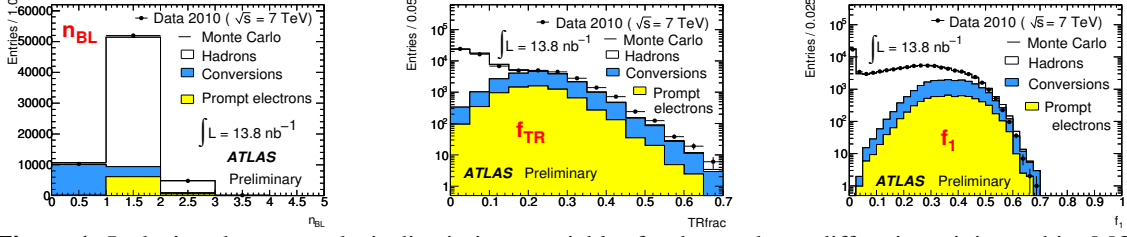


Figure 1: Inclusive electron analysis discriminant variables for data and non-diffractive minimum bias MC.

1. Introduction

Efficient reconstruction of electromagnetic (EM) objects, electrons and photons, with a small background is crucial to many of the physics results of interest at the LHC. This note reports some early results on EM object reconstruction with ATLAS at $\sqrt{s} = 7$ TeV, including a measurement of the inclusive electron p_T spectrum and the observation of prompt photons and J/ψ mesons.

ATLAS is fully described in [1]; here, we draw attention to a few relevant details. The innermost pixel layer of the central tracker is at $r \sim 5$ cm and is useful for rejecting conversions. The outermost tracking detector is the transition radiation tracker (TRT), consisting of straw tubes interleaved with polypropylene radiators; it provides good discrimination between electrons and pions of energies 1–200 GeV. The EM calorimeter uses Pb/liquid Ar with an accordion geometry and fine segmentation. Within $|\eta| < 2.5$, there are three longitudinal layers; the first (layer 1) is finely segmented in η (up to 0.003), allowing precise η measurements and rejection of π^0 decays.

EM object reconstruction starts by finding seed clusters in the EM calorimeter with significant energy; these can be defined either with a (η, ϕ) window or with a nearest-neighbor clustering algorithm. They are matched with tracks; on the basis of this, each candidate is classified as either an electron, a photon, or a converted photon. A final cluster is formed from cells in a rectangular region around the seed, and the measurements from the tracker and calorimeter are combined.

2. Inclusive electron analysis

This analysis [2] measures the inclusive p_T spectrum of electron candidates and breaks down the contributions to this by source, either $b/c \rightarrow e$ (Q), conversions (γ), or hadrons (h). We require $E_T > 7$ GeV, $|\eta| < 2.0$ and make additional requirements on f_1 , the fractional energy in layer 1; the shower width and shape in layer 1; the track’s impact parameter with respect to the event vertex and number of hits; and $\Delta\eta(\text{track}, \text{cluster})$. This selection yields 67124 events in 13.8 nb^{-1} .

We decompose the sample using the “matrix method,” exploiting the differing efficiencies of each source to pass selections on discriminating variables (Fig. 1). f_{TR} , the fraction of TRT hits passing a high threshold, discriminates between electrons and hadrons; f_1 is used as a cross-check. To discriminate between electrons and conversions, we use n_{BL} , the number of hits in the innermost (B) pixel layer; conversions usually occur outside this layer. We find the efficiencies for samples Q and γ using Monte Carlo (MC) simulations; for h , we use data with an inverted f_1 selection. Our observed prompt electron signal (Table 1, Fig. 2) is 9920 ± 160 (stat.) ± 990 (syst.) events.

3. Prompt photon analysis

This analysis [4] reconstructs prompt, isolated photons and measures the purity of the sample.

| | Data | MC |
|----------|-----------------|-----------------|
| h | 43470 ± 240 | 46730 ± 150 |
| γ | 13160 ± 150 | 13580 ± 80 |
| Q | 9920 ± 160 | 6890 ± 60 |
| Total | 67124 | |

Table 1: Decomposition of the inclusive electron sample by component, compared to PYTHIA [3].

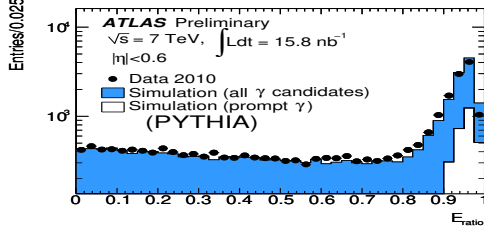


Figure 3: (left) E_{ratio} , the asymmetry between the first two maxima in layer 1. (right) Photon isolation.

| E_T (GeV) | N_{cand} | Purity (%) | N_{sig} |
|----------------|-------------------|-------------------|-------------------------|
| 10–15 | 5271 | $24 \pm 5 \pm 24$ | $1289 \pm 297 \pm 1362$ |
| 15–20 | 1213 | $58 \pm 5 \pm 8$ | $706 \pm 69 \pm 86$ |
| > 20 | 864 | $72 \pm 3 \pm 6$ | $618 \pm 42 \pm 59$ |

Table 2: Total photon candidates and purity and number of signal events in the signal region.

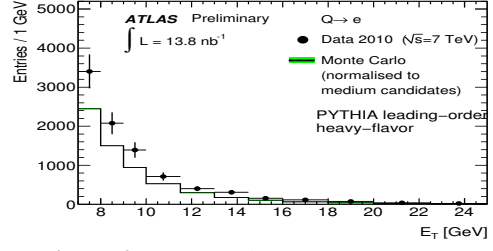


Figure 2: Prompt electron E_T spectrum.

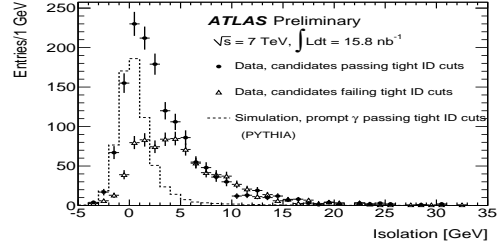
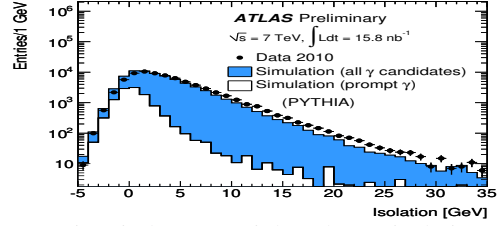


Figure 4: γ candidate isolation, $E_T > 20$ GeV.

Our initial selection requires photon candidates with $E_T > 10$ GeV and $|\eta| < 2.37$, yielding 268992 events in 15.8 nb^{-1} . We then require small leakage out the back of the EM calorimeter, small width in calorimeter layer 2, and large $R_\eta = E(3 \times 7)/E(7 \times 7)$, which also indicates a narrow cluster.

Two more requirements define our final sample. First, tight cuts on the cluster shape and width in layer 1 which select prompt photons and reject π^0 decays. Figure 3, left, shows one such variable. Second, isolation: the energy sum within $R < 0.4$ around the candidate must be < 3 GeV (Fig. 3, right). We find the sample purity by counting the number of candidates that pass each of the four combinations of the cluster shape and isolation selections. Assuming that these selections are uncorrelated and that the amount of prompt photon signal outside of the signal region is negligible, the signal and background fractions in the signal region may be calculated. (We use simulations to correct for the failure of these assumptions to hold exactly.) Results are in Table 2 and Fig. 4. A prompt photon signal is seen for $E_T > 15$ GeV, with purity over 70% for $E_T > 20$ GeV.

4. J/ψ analysis

This analysis [5] uses 77.8 nb^{-1} and reconstructs a J/ψ mass peak, using it to measure the shapes of some of the discriminating variables. For improved efficiency at low E_T , this analysis uses nearest-neighbor, rather than rectangular, cluster seeds. We select opposite-sign pairs of electron candidates, one with $E_T > 4$ GeV and one with $E_T > 2$ GeV. We make further selections on R_η , f_1 , the cluster's shape in layer 1, and the track impact parameter, number of hits, and f_{TR} .

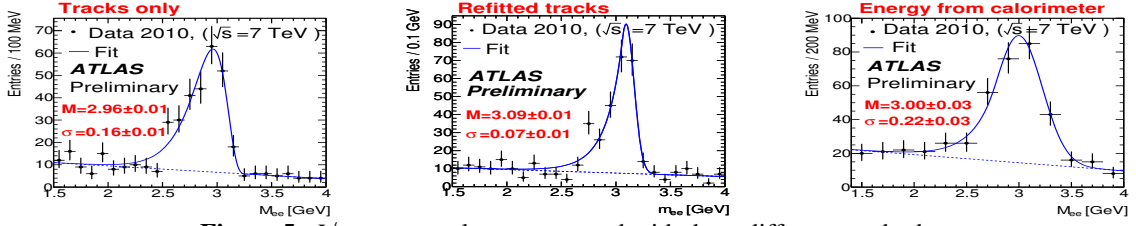


Figure 5: J/ψ mass peak reconstructed with three different methods.

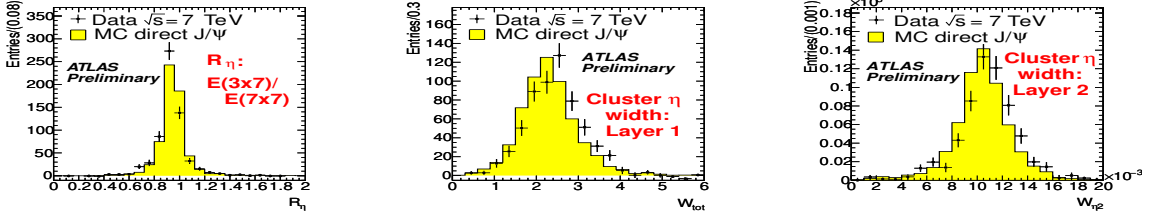


Figure 6: Electron discriminant variables from electrons from J/ψ decay, compared to PYTHIA.

We calculate the J/ψ mass in three ways. First, using kinematics from tracks only (Fig. 5, left). This gives a mass of 2.96 ± 0.01 GeV, slightly low compared to the Particle Data Group value of 3.097 GeV [6]. This is expected, since this method ignores energy losses due to bremsstrahlung. Second, taking into account the energy loss by bremsstrahlung in the tracker material. This (Fig. 5, middle) yields 3.09 ± 0.01 GeV. Third, taking energies from the calorimeter clusters and directions from the tracks. This gives (Fig. 5, right) 3.00 ± 0.03 GeV, also slightly low, as the current calorimeter energy calibrations are known to be suboptimal at these low cluster energies.

The J/ψ peak defines real electrons that can be used to check the detector simulation. We perform a “tag-and-probe” analysis: we maintain tight selections on one, *tag*, candidate, and remove the shower shape selections from the other, *probe*, candidate. We then select candidate pairs with masses within 2.7–3.2 GeV and $f_1 > 0.15$ and plot variables from the probe. There is general agreement between data and the simulation (Fig. 6); however, statistics now available reveal some small systematic differences in lateral shower shapes. Work is in progress on understanding these.

5. Conclusions

ATLAS and the LHC are performing well; the luminosity is increasing rapidly, and we will soon have large electron samples from both J/ψ and W/Z decays. We are working to better understand the detector performance in preparation for new discoveries in electron/photon channels.

This work is supported in part by the U.S. Department of Energy under contract DE-AC02-98CH10886 with Brookhaven National Laboratory.

References

- [1] ATLAS Collaboration, *JINST* **3** (2008) S08003.
- [2] ATLAS-CONF-2010-073 (2010) [<http://cdsweb.cern.ch/record/1281364>].
- [3] T. Sjöstrand et al., *Comp. Phys. Comm.* **135** (2001) 238.
- [4] ATLAS-CONF-2010-077 (2010) [<http://cdsweb.cern.ch/record/1281368>].
- [5] atlas.web.cern.ch/Atlas/GROUPS/PHYSICS/EGAMMA/PublicPlots/20100721/ATL-COM-PHYS-2010-518/index.html
- [6] K. Nakamura et al. (Particle Data Group), *J. Phys. G* **37**, 075021 (2010).